HHS Public Access

Author manuscript

Dev Neurosci. Author manuscript; available in PMC 2015 November 09.

Published in final edited form as:

Dev Neurosci. 2015 ; 37(0): 407–416. doi:10.1159/000381704.

In vivo Monitoring of Cerebral Hemodynamics in the Immature Rat: Effects of Hypoxia-Ischemia and Hypothermia

Erin M. Buckley[a], **Shyama D. Patel**[b], **Benjamin F. Miller**[a], **Maria Angela Franceschini**[a], and **Susan J. Vannucci**[b]

[a]Department of Radiology, Athinoula A. Martinos Center for Biomedical Imaging, Massachusetts General Hospital, Charlestown, Mass

[b]Department of Pediatrics/Newborn Medicine, Weill Cornell Medical College, New York, N.Y., USA

Abstract

Background—Neonatal hypoxic-ischemic (HI) encephalopathy occurs in 1–4 per 1,000 live term births and can cause devastating neurodevelopmental disabilities. Currently, therapeutic hypothermia (TH) is the only treatment with proven efficacy. Since TH is associated with decreased cerebral metabolism and cerebral blood flow (CBF), it is important to assess CBF at the bedside. Diffuse correlation spectroscopy (DCS) has emerged as a promising optical modality to noninvasively assess an index of CBF (CBF_i) in both humans and animals. In this initial descriptive study, we employ DCS to monitor the evolution of CBF_i following HI with or without TH in immature rats. We investigate potential relationships between CBF and subsequent cerebral damage.

Methods—HI was induced on postnatal day 10 or 11 rat pups by right common carotid artery ligation followed by 60–70 min hypoxia (8% oxygen). After HI, the pups recovered for 4 h under hypothermia (HI-TH group, n = 23) or normothermia (HI-N group, n = 23). Bilateral measurements of hemispheric CBF_i were made with DCS in unanesthetized animals at baseline, before HI, and 0, 1, 2, 3, 4, 5, and 24 h after HI. The animals were sacrificed at either 1 or 4 weeks, and brain injury was scored on an ordinal scale of 0–5 (0 = no injury).

Results—Carotid ligation caused moderate bilateral decreases in CBF_i. Following HI, an initial hyperemia was observed that was more prominent in the contralateral hemisphere. After initiation of TH, CBF_i dropped significantly below baseline levels and remained reduced for the duration of TH. In contrast, CBF_i in the HI-N group was not significantly decreased from baseline levels. Reductions in CBF_i after 4 h of TH were not associated with reduced damage at 1 or 4 weeks. However, elevated ipsilateral CBF_i and ipsilateral-to-contralateral CBF_i ratios at 24 h were associated with worse outcome at 1 week after HI.

Conclusions—Both HI and TH alter CBF_i, with significant differences in CBF_i between hypothermic and normothermic groups after HI. CBF_i may be a useful biomarker of subsequent cerebral damage.

Erin M. Buckley, Massachusetts General Hospital, 13th St., Building 149, Charlestown, MA 02129 (USA), ebuckle2@gmail.com.

Keywords

Cerebral blood flow; Hypoxic-ischemic encephalopathy; Therapeutic hypothermia; Diffuse correlation spectroscopy

Introduction

Neonatal hypoxic-ischemic encephalopathy (HIE) occurs in 1–4 per 1,000 live term births and can lead to devastating lifelong motor, cognitive and behavioral disabilities [1, 2]. In both asphyxiated infants and experimental animal models, hypoxia-ischemia (HI) of sufficient duration to cause a significant decrease in cerebral blood flow (CBF) to the fetal brain results in a depletion of cerebral high-energy phosphates in vulnerable brain regions, generating a primary energy failure. Although postasphyxial resuscitation and reperfusion initially promotes recovery of the energy state, studies employing phosphorus magnetic resonance spectroscopy in newborn infants and experimental animals demonstrate a biphasic pattern of energy failure, including a secondary energy failure occurring 6–15 h after the initial HI event [3, 4]. It is likely that this interval represents a therapeutic window during which neuroprotective interventions may prevent the cascade of neuroexcitotoxic events that lead to secondary energy failure and irreversible cell death [1, 2, 5]. Currently, therapeutic hypothermia (TH), initiated within 6 h of birth, is the only such intervention clinically available that results in significantly reduced mortality and morbidity in these children [6, 7]. However, many questions still exist regarding the selection of candidates for TH and the optimal degree and duration of hypothermia [1].

Despite the possible involvement of other mechanisms, successful treatment with TH is associated with decreased cerebral metabolism and CBF [8–10]. Thus, a noninvasive modality capable of assessing these parameters at the bedside may be an invaluable tool for therapy monitoring and prognosis of HIE. Diffuse correlation spectroscopy (DCS) has emerged over the past 15 years as a promising optical modality that measures cerebral hemodynamics in a noninvasive manner using near-infrared light without the use of external contrasts [11–13]. The technique is similar to laser speckle contrast imaging and laser Doppler flowmetry in that it provides an index of CBF (CBF_i) that is highly correlated with absolute CBF [14, 15]. However, unlike these techniques, DCS works in the multiple-light scattering realm, thus making it sensitive to deeper tissue CBF without the need for thinning or removal of the skull [16–19]. Because of its greater depth penetration, DCS has been applied extensively in human neonates at the bedside to describe CBF_i changes with postmaturational age and with various clinical interventions [for a recent review, see 16].

The Vannucci model of unilateral carotid occlusion followed by hypoxia is often used to investigate mechanisms of injury and therapeutic strategies for neonatal HIE [20]. Recent investigations in this model have demonstrated protective effects of TH after HI. However, the cerebral hemodynamic effects of this therapy have yet to be elucidated. In this initial descriptive study, we employ DCS to monitor alterations in CBF_i following HI, with or without TH therapy, in this well-established neonatal rat model of HI.

Methods

Dated pregnant Wistar rats were purchased from Charles River Laboratories at embryonic day 15, housed individually, and allowed to deliver vaginally. On the day of birth (P1), the pups were randomized and reassigned to the dams in groups of 10, with approximately equal numbers of males and females when possible. All procedures described were approved by the Weill Cornell Medical College and the Massachusetts General Hospital animal care and use committee.

Induction of HI and Hypothermia

Unilateral cerebral HI was induced in rat pups using the Vannucci model as previously described [20] and recently modified for use in the P10/P11 rat pup as representative of the full-term infant brain [21, 22]. The study protocol is depicted in figure 1a. In brief, the animals were anesthetized with 3–5% isoflurane, and the right common carotid artery was permanently ligated. After ligation, the pups were returned to the dam for 2 h before being transferred to a temperature-controlled chamber (35.5 ° C) where they were exposed to 60–70 min of hypoxia (8% oxygen/balance nitrogen). Following HI, the animals were randomly assigned to one of two groups to recover for 4 h either under hypothermia (HI-TH), achieved by placing pups in open glass jars submerged in a circulating water bath (29–30 ° C, target rectal temperature 32 ° C) or under normothermia (HI-N) in the original 35.5 ° C chamber; rectal temperatures were recorded hourly. At the end of 4 h, the pups were rewarmed and returned to the dam. Nonoperated control pups were separated from the dam in a temperature-controlled chamber (35.5 ° C) for the same duration as the HI-N and HI-TH pups.

Cerebral Blood Flow Index

Measurements of CBF_i were made using DCS, a relatively new technology. DCS uses near-infrared light to noninvasively probe dynamic optical properties of cortical brain tissue vasculature. DCS measures temporal fluctuations in reflected near-infrared light intensity on the tissue surface, which are primarily caused by moving red blood cells. A temporal intensity autocorrelation function is used to quantify these intensity fluctuations. This autocorrelation function is then fit to simple models in order to derive a tissue CBF_i (mm^2/s) [11–13]. Previous studies in both animals and humans have shown that absolute CBF_i, as well as relative changes in CBF_i over time, are strongly correlated with CBF measured by other techniques, including fluorescent microspheres, Xenon-CT, laser Doppler flowmetry, bolus tracking time domain near-infrared spectroscopy, arterial spin-labeled and phase-encoded velocity mapping magnetic resonance imaging, and transcranial Doppler ultrasound [for a recent review of DCS validation studies, see 23].

DCS measurements of CBF_i were made in awake, unanesthetized rats by gently holding the DCS sensor over each hemisphere (fig. 1b). A custom-built DCS instrument was employed that used either a 785- or 852-nm-long coherence length laser (CrystaLaser, Reno, Nev., USA), a photon-counting avalanche photodiode (PerkinElmer, Vaudreuil-Dorion, Que., Canada), and a hardware autocorrelator board (www.correlator.com). For these experiments, a single-source detector pair (6-mm separation) was embedded in a rigid black sensor. Given

the relatively short distance to the brain in the P10/P11 rat (<0.5 mm), this separation was sufficient to probe cortical brain tissue (fig. 1c). For each DCS measurement session, 5 s of 1 Hz acquisition of intensity autocorrelation functions were acquired over each hemisphere in sequence. Measurements were repeated up to 3 times over both hemispheres to account for local inhomogeneities under the optical sensor. DCS repeatability was assessed by obtaining as many as 10 repetitions in a small subset of animals. Data was fit to the semi-infinite homogenous solution to the correlation diffusion equation, assuming a fixed, wavelength-dependent value for the absorption and reduced scattering coefficients, $\mu_a(\lambda)$ and $\mu_s'(\lambda)$, respectively, of 0.1 and 4.1 cm^{-1} at 852 nm and 0.1 and 5.6 cm^{-1} at 785 nm.

DCS data was rejected according to the following objective criteria (similar to those described by Roche-Labarbe et al. [24]). First, we discarded intensity autocorrelation curves for which the tail of the curve differed from 1 by more than 0.005, indicating movement of the animal during the 1-second averaging time. Second, after removing any outliers within a given repetition, we discarded repetitions with a coefficient of variation (CoV, standard deviation:mean) greater than 20%, again indicative of animal movement. Finally, we only included measurement sessions for which the average hemispheric CBF_i across multiple repetitions had a CoV less than 20 %.

As shown by black arrows in figure 1a, DCS data was obtained at the following time points: baseline prior to anesthesia induction, after ligation following 2 h recovery with the dam (before HI), and 0, 1, 2, 3, 4, 5, 24, and 48 h after HI. Only a subset of pups was measured at the 48-hour time point. In addition to these time points, control animals were also measured once daily from P8 to P13 to quantify changes in CBF_i with postnatal age. Measurements were not made during HI, as the animals were in a closed chamber and not accessible to measurements. Total DCS measurement duration per pup did not exceed 2 min.

Relative change in CBF_i from baseline in each hemisphere at a given time point, ΔrCBF(t), was calculated as follows:

$$\Delta rCBF(t) = \frac{CBF_i(t) - CBF_{i,bl}}{CBF_{i,bl}} \times 100\%,$$

where the subscript *bl* denotes baseline CBF_i.

Systemic Hemodynamics

Heart rate and transcutaneous oxygen saturation (SpO_2) were measured using a MouseOx small animal oximeter (STARR Life Sciences Corp., Oakmont, Pa., USA). These measurements were made after each DCS measurement session. The unanesthetized animal was gently manually restrained and a collar clip was placed around the neck to capture instantaneous values of heart rate and SpO_2.

Brain Injury

The animals were sacrificed at either 1 or 4 weeks after HI to assess cerebral injury. Brains were removed and sliced into serial 2-mm coronal sections treated either with tetrazolium

chloride (1-week outcomes) or formaldehyde (4-week outcomes) for gross morphometry of individual hemispheres and extent of infarct. Injury, described as a damage score, in two anterior (caudate + putamen) and two posterior (hippocampal + thalamus) sections was rated on an ordinal scale of 0–4 as previously described (0 = no damage, 1 = mild atrophy only, 2 = atrophy and ventriculomegaly, 3 = 10–25% ipsilateral volume loss, and 4 >25% ipsilateral volume loss) [21, 25]. A score of 5 was given if the animal was ahemispheric (only seen at 4 weeks). Scores for the anterior and posterior sections were averaged to assess a global damage score.

Statistical Analysis

Data are reported as means (with standard error of the mean, SEM) unless otherwise stated. Paired t tests were used to determine whether CBF_i at each time point differed from baseline levels. Unpaired t tests were used to test for significant differences between HI-N, HI-TH and control groups (controls only tested at the 24-hour time point). Spearman's rank-based nonparametric approach was employed to test for associations between CBF_i, ΔrCBF and ipsilateral-to-contralateral CBF_i ratio with subsequent 1- and 4-week injury scores. All analyses were performed using MATLAB and Statistics Toolbox Release 2013b (MathWorks Inc., Natick, Mass., USA). Associated p values represent the significance of two-sided tests. Statistical significance was declared for p values <0.05.

Results

A total of 48 immature rats from 5 litters were subjected to HI (28 male and 20 female), and 24 pups from 3 litters were used as controls; 2 pups died during HI, leaving a final cohort of 23 pups subjected to HI followed by normothermia (HI-N) and 23 subjected to HI followed by TH (HI-TH). A third pup from the HI-N group died 2 weeks after HI. All HI-TH pups reached the target rectal temperature of 30–32 ° C; the HI-N pups averaged rectal temperatures of 37.6 ° C during the same 4-hour interval.

A total of 966 average hemispheric CBF_i measurements were taken with DCS on the 48 HI animals. Approximately 9% of these measurements were discarded based on the objective criteria described above. The average intrahemispheric CoV for each measurement session, which consisted of 2–3 repetitions, was 11.4% (SEM 0.1%).

CBF: Before HI

Baseline CBF_i was tightly distributed amongst the 48 HI pups; values ranged from 0.46 to 0.83×10^{-5} mm^2/s and had a mean (standard deviation) of 0.65 (SEM 0.08) $\times 10^{-5}$ mm^2/s. Baseline CBF_i did not differ between males and females, between litters or between groups ($p > 0.05$, data not shown). Hemispheric differences were not observed, i.e. the mean right-to-left CBF_i ratio was 1.05 (SEM 0.17).

At 2 h after right carotid ligation, ipsilateral CBF_i was significantly decreased by 19% (SEM 3%) ($p < 0.001$, data not shown). CBF_i was also minimally reduced in the contralateral hemisphere by 6% (SEM 3%; $p = 0.009$). As expected, ligation affected CBF_i in the ipsilateral hemisphere more than the contralateral hemisphere, leading to a ratio of

ipsilateral-to-contralateral CBF_i of 0.91 (SEM 0.03), which was significantly different from unity. Both sexes responded similarly to ligation.

CBF: After HI

CBF_i measurements were made in all animals sequentially, starting immediately at the restoration of normoxia and continuing through the following 25 min. Contralateral CBF_i in most animals was substantially increased during the initial 6 min of recovery compared to both baseline and pre-HI levels and decreased thereafter. Although CBF_i in the ipsilateral hemisphere was also increased compared to pre-HI levels, the magnitude of these increases was significantly less than the contralateral hemisphere (fig. 2), resulting in a mean ipsilateral-to-contralateral CBF_i ratio of 0.83 (SEM 0.04; $p < 0.001$) at this immediate post-HI time point (fig. 2, 3; table 1).

The animals assigned to the HI-TH group were then placed in cooling chambers for 4 h; rectal temperature and CBF_i were monitored hourly. The animals assigned to normothermic recovery were maintained in a normothermic chamber and monitored similarly for the same duration. In those animals exposed to TH, CBF_i in both hemispheres decreased from immediate post-HI values to below both baseline and pre-HI levels and remained reduced by approximately 30% of baseline levels for the duration of TH (fig. 3a–d; table 1). In contrast, during this same 4-hour recovery period, CBF_i in the HI-N group was significantly elevated compared to pre-HI levels (more so in the contralateral than ipsilateral hemisphere); CBF_i was not significantly different from baseline levels in either hemisphere on average. In both the HI-TH and HI-N groups, ipsilateral CBF_i was lower than contralateral CBF_i, but the ratio of ipsilateral-to-contralateral CBF_i approached unity over time, especially in the HI-TH group (fig. 3e; table 1).

Following the 4-hour experimental interval, the pups were returned to their dams. After 1 h (5 h after HI), CBF_i in the HI-TH group had on average returned to baseline levels in both hemispheres. CBF_i in the HI-N group remained unchanged from the 4-hour interval (fig. 3; table 1).

At 24 h, both ipsilateral and contralateral CBF_i values were increased above baseline in HI-N pups, while comparable measurements in the HI-TH pups were little changed from baseline (fig. 3; table 1). Because CBF_i increases significantly during normal maturation in neonatal rats (fig. 4), we also compared 24-hour data to normal controls that were separated from the dam for similar durations as HI-N and HI-TH pups. No significant differences in relative increase in CBF_i at 24 h from baseline were observed between the HI-N or HI-TH groups and controls. However, the average relative increase in ipsilateral CBF_i in the HI-N group of 40% (SEM 10%) was higher than that of 20% (SEM 6%) in controls ($p = 0.11$, data not shown). Additionally, in both the HI-N and HI-TH groups, the average ipsilateral-to-contralateral CBF_i ratios were higher than controls ($p = 0.08$ and 0.03, respectively), who had an average right-to-left CBF_i ratio of 0.94 (SEM 0.01).

Heart Rate and Transcutaneous SpO_2

Heart rate and SpO_2 were measured in a subset of 18 animals (n = 9 HI-N, n = 9 HI-TH). Baseline and pre-HI measurements were taken in only 6 animals, whereas all 18 animals

were measured at the post-HI time points. Systemic circulation remained well oxygenated throughout the duration of the experiment. Mean SpO_2 for both groups remained at or above 98% at all time points (data not shown).

Baseline heart rate had a mean of 396 beats per min (bpm; SEM 23). At 30 min after HI, the heart rate was elevated from baseline in both the HI-TH and HI-N groups to 421 bpm (SEM 17) and 466 bpm (SEM 8), respectively. In the HI-N group, the heart rate stayed elevated for the duration of the 4-hour post-HI recovery period, with a mean value over the 4-hour period of 465 bpm (SEM 5; $p < 0.001$). In contrast, heart rates in the HI-TH group during the 4-hour recovery period remained at baseline levels on average and were significantly lower than the HI-N group at 377 bpm (SEM 6) compared to HI-N ($p < 0.001$). By 5 h after HI, after the 1-hour recovery with the dam (and rewarming in the HI-TH group), the heart rate was similar amongst both groups, with a mean of 406 bpm (SEM 21) in the HI-N group and 386 bpm (SEM 18) in the HI-TH group, and it remained stable at baseline levels through 48 h.

Brain Injury

Animals in the HI-TH group demonstrated significant neuroprotection relative to the HI-N group at both the 1-and 4-week post-HI study end points ($p = 0.001$). At 1-week post-HI the median (interquartile range, IQR) injury score in the HI-TH group was 1.5 (1–3), whereas the HI-N group was 4 (2.5–4). At 4 weeks after HI the HI-N and HI-TH injury scores were 1 (0–2) and 3 (1.5–5), respectively.

We initially focused on potential relationships between CBF_i, ΔrCBF and ipsilateral-to-contralateral CBF_i ratios at 4 and 24 h after HI with subsequent injury scores. Since damage scores were assessed at either 1 or 4 weeks after HI, relationships between hemodynamics and outcome were explored for each outcome time point independently. Ipsilateral CBF_i and ipsilateral-to-contralateral CBF_i ratio at 24 h after HI were the most promising predictors of worse 1-week injury scores when looking at all animals regardless of treatment paradigm ($p = 0.009$ and 0.030, respectively; fig. 5a, b). When a similar analysis was performed on the subset of animals with 4-week injury scores, these trends were not significant ($p > 0.05$; fig. 5c, d), although it is likely that this group was underpowered.

Discussion

In this initial descriptive study, we employed DCS to monitor cerebral hemodynamics in neonatal rats following unilateral cerebral HI treated with and without TH. While a handful of studies have been conducted to quantify CBF before, during and after HI in neonatal rats, this is the first study to demonstrate the effects of TH on CBF. DCS has several advantages over the relatively few other techniques that have been used to quantify cerebral hemodynamics in neonatal rats in the past. Animals do not have to be sacrificed for DCS measurements, as is the case for radioisotopic measurements. DCS measurements can be done on awake, unanesthetized animals, as opposed to laser Doppler flowmetry, laser speckle imaging, perfusion magnetic resonance imaging, and Doppler ultrasound, which require sedation that can alter cerebral hemodynamics. Furthermore, DCS has been used

successfully in human neonates. Thus, results obtained in animals can be directly translated to the clinic.

Following carotid ligation, we observed a 20% decrease in CBF_i in the ipsilateral hemisphere, suggesting that collateral circulation from the circle of Willis, and cerebral autoregulatory mechanisms were not sufficient to completely restore perfusion. The contralateral hemisphere also exhibited a small (~5%) yet significant decrease in CBF_i on average. Other investigators have observed similar reductions in flow after ligation in neonatal and adult rats [26–28]. We highlight that although CBF_i was reduced, it is most likely still above critical levels needed for metabolic demand, given that carotid ligation alone does not produce cell damage in neonatal rats [29].

Immediately after HI, hyperemia, i.e. a significant increase in CBF_i from both baseline and postligation levels, was present in both hemispheres, although it was more pronounced in the contralateral side. This effect subsided within 5–10 min. Hyperemia is commonly seen in other neonatal animal models following HI [30–33], and it was seen in internal carotid arteries (macrovasculature) in a cohort of P7 rats [34]. However, hyperemia has not been observed in the handful of studies in neonatal rats that report microvascular CBF measured immediately after HI [27, 35]. The discrepancy between our findings and these other studies may arise from the severity of the HI insult and/or from differences in the sensitivities of the techniques used to assess CBF. Both of these reports employed a hypoxia duration that was 2–3 times longer than our current experiment, as well as younger animals (P7 vs. P10/P11).

During the initial 4 h of recovery, CBF_i was elevated in the HI group compared to pre-HI levels in both hemispheres. However, hypothermia blunted this elevation and led to a significant reduction in CBF_i compared to both pre-HI and baseline levels. These results agree well with the small handful of studies that have investigated the effects of hypothermia on CBF following neonatal HI [9, 36–38], and most likely reflect the reductions in cerebral metabolic rate that occur with cooling.

By 24 h after HI, ipsilateral CBF_i was elevated in the HI-N group compared to HI-TH animals ($p < 0.05$) and controls ($p = 0.11$). These observations could either reflect real alterations in cerebral hemodynamics associated with secondary energy failure and worse outcome [39] or they could be due to an experimental artifact such as increasing edema (see Limitations).

We did not observe any statistically significant relationships between absolute CBF_i at 4 h after HI and subsequent infarct scores at 1 or 4 weeks. However, 24-hour post-HI ipsilateral CBF_i and ipsilateral-to-contralateral CBF_i ratios were positively correlated with 1-week damage scores. A handful of other publications have investigated the relationship between CBF and brain injury in the immature rat subjected to HI. Ohshima et al. [27] saw a weak positive relationship between the ratio of ipsilateral-to-contralateral CBF at 6 h after HI and the ratio of ipsilateral-to-contralateral brain volume loss. Char riaut-Marlangue et al. [34] observed a strong significant positive correlation between the relative change in CBF velocity in the internal carotid artery minutes after HI and subsequent tissue loss measured with cresyl-violet staining. The lack of a strong relationship between our 4- and 24-hour

post-HI measurements of CBF_i and 4-week damage scores suggests that CBF_i alone may not be a sufficient predictor of ultimate damage. Tichauer et al. [40] demonstrated that the cerebral metabolic rate of oxygen ($CMRO_2$), *not* CBF, was most sensitive to insult severity in a newborn piglet model of HI. The authors postulate that impaired cerebral autoregulation may lead to an uncoupling of $CMRO_2$ from CBF, thus explaining the relative insensitivity of CBF to insult severity. Thus, future work will combine DCS measures of CBF_i with oxygen extraction, measured by near-infrared spectroscopy or invasive blood draws, in order to quantify an index of $CMRO_2$.

Limitations

Although DCS enables the noninvasive quantification of CBF_i without the use of sedation, the technique is limited in spatial resolution. The measured CBF index represents a bulk average of the cortical tissue underneath the optical sensor. The technique is also highly sensitive to motion artifacts, which are more prevalent when monitoring awake animals. In future experiments, due to recent improvements in the DCS acquisition software that allow for integration times in the order of 100 ms, we will be able to eliminate measured intensity autocorrelation functions that demonstrate obvious motion artifacts. Furthermore, the technique is sensitive to signal contributions from extracerebral layers since a simple semi-infinite geometry was used to fit the data. Future work will benefit from modeling of these layers to isolate signal contributions from cortical tissue. Nevertheless, even with small motion artifacts and potential extracerebral signal contributions, the average CoV was 11%, suggesting that these effects do not dominate our results.

The assumption of a fixed value for the tissue-reduced scattering coefficient can have a significant impact on the resultant CBF_i. We assumed a fixed value of $\mu_s'(\lambda)$ for all rats across all time points. These assumptions are somewhat justified because our cohort was relatively homogenous, and the animals did not have significant blood loss (which would change the density of scatterers) following the insult. However, Mujsce et al. [35] did observe significant edema in the ipsilateral hemisphere in P7 rats by 4 h after HI and continuing through 24 h, and if these effects were also present in our cohort of P10/P11 rats, intracellular swelling could lead to increases in $\mu_s'(\lambda)$ that we did not account for in our model for CBF_i. Therefore, our CBF_i values at 4, 5 and 24 h after HI in the ipsilateral hemisphere may be artificially elevated. Future experiments would benefit from the concurrent use of a time or frequency domain near-infrared spectroscopy device to quantify $\mu_s'(\lambda)$ for each animal at each measurement time point and to input these measurements into the intensity autocorrelation function fit for CBF_i.

Conclusions

TH resulted in significant reductions in CBF in a neonatal rat model of HI. Although hypothermia therapy improves brain injury following HI, we did not observe a relationship between CBF_i during treatment and subsequent damage score. However, elevated ipsilateral CBF_i and ipsilateral-to-contralateral CBF_i ratios at 24 h were positively associated with injury score at 1 week.

Acknowledgments

We would like to thank Dr. P. Ellen Grant for support and helpful discussions, Dr. Ivy Lin for help with optical probe construction, Alexandria Hutton for expert technical assistance, Dr. Stefan Carp for assistance with DCS acquisition software, and Dr. Robert C. Vannucci for helpful discussion and critical review of the manuscript. We would also like to gratefully acknowledge support from the National Institutes of Health through grant No. R01-EB001954 (M.A. Franceschini, principal investigator) and R21NS083425 (S.J. Vannucci, principal investigator), the Fondation Leducq Transatlantic Network for Neonatal Stroke (S.J. Vannucci) and the MGH ECOR Fund for Medical Discovery Postdoctoral Fellowship Award (E.M. Buckley, principal investigator).

References

1. Gunn AJ. Cerebral hypothermia for prevention of brain injury following perinatal asphyxia. Curr Opin Pediatr. 2000; 12:111–115. [PubMed: 10763759]
2. Vannucci RC, Perlman JM. Interventions for perinatal hypoxic-ischemic encephalopathy. Pediatrics. 1997; 100:1004–1114. [PubMed: 9374573]
3. Azzopardi D, Wyatt JS, Hamilton PA, Cady EB, Delpy DT, Hope PL, Reynolds EO. Phosphorus metabolites and intracellular pH in the brains of normal and small for gestational age infants investigated by magnetic resonance spectroscopy. Pediatr Res. 1989; 25:440–444. [PubMed: 2717258]
4. Lorek A, Takei Y, Cady EB, Wyatt JS, Penrice J, Edwards AD, Peebles D, Wylezinska M, Owen-Reece H, Kirkbride V, et al. Delayed ('secondary') cerebral energy failure after acute hypoxia-ischemia in the newborn piglet: continuous 48-hour studies by phosphorus magnetic resonance spectroscopy. Pediatr Res. 1994; 36:699–706. [PubMed: 7898977]
5. Gunn AJ, Gunn TR. The 'pharmacology' of neuronal rescue with cerebral hypothermia. Early Hum Dev. 1998; 53:19–35. [PubMed: 10193924]
6. Azzopardi DV, Strohm B, Edwards AD, Dyet L, Halliday HL, Juszczak E, Kapellou O, Levene M, Marlow N, Porter E, Thoresen M, Whitelaw A, Brocklehurst P. Moderate hypothermia to treat perinatal asphyxial encephalopathy. New Engl J Med. 2009; 361:1349–1358. [PubMed: 19797281]
7. Shankaran S, Pappas A, McDonald SA, Vohr BR, Hintz SR, Yolton K, Gustafson KE, Leach TM, Green C, Bara R, Huitema CMP, Ehrenkranz RA, Tyson JE, Das A, Hammond J, Peralta-Carcelen M, Evans PW, Heyne RJ, Wilson-Costello DE, Vaucher YE, Bauer CR, Dusick AM, Adams-Chapman I, Goldstein RF, Guillet R, Papile L-A, Higgins RD. Childhood outcomes after hypothermia for neonatal encephalopathy. New Engl J Med. 2012; 366:2085–2092. [PubMed: 22646631]
8. Liu L, Yenari MA. Therapeutic hypothermia: neuroprotective mechanisms. Front Biosci. 2007; 12:816–825. [PubMed: 17127332]
9. Wintermark P, Hansen A, Gregas MC, Soul J, Labrecque M, Robertson RL, Warfield SK. Brain perfusion in asphyxiated newborns treated with therapeutic hypothermia. AJNR Am J Neuroradiol. 2011; 32:2023–2029. [PubMed: 21979494]
10. Yenari MA, Han HS. Neuroprotective mechanisms of hypothermia in brain ischaemia. Nat Rev Neurosci. 2012; 13:267–278. [PubMed: 22353781]
11. Boas DA, Campbell LE, Yodh AG. Scattering and imaging with diffusing temporal field correlations. Phys Rev Lett. 1995; 75:1855–1858. [PubMed: 10060408]
12. Boas DA, Yodh AG. Spatially varying dynamical properties of turbid media probed with diffusing temporal light correlation. J Opt Soc Am A. 1997; 14:192–215.
13. Durduran T, Choe R, Baker WB, Yodh AG. Diffuse optics for tissue monitoring and tomography. Rep Prog Phys. 2010; 73:43.
14. Diop M, Verdecchia K, Lee T, St Lawrence K. Calibration of diffuse correlation spectroscopy with a time-resolved near-infrared technique to yield absolute cerebral blood flow measurements. Biomed Opt Express. 2011; 2:2068–2081. [PubMed: 21750781]
15. Jain V, Buckley EM, Licht DJ, Lynch JM, Schwab PJ, Naim MY, Lavin NA, Nicolson SC, Montenegro LM, Yodh AG, Wehrli FW. Cerebral oxygen metabolism in neonates with congenital heart disease quantified by MRI and optics. J Cereb Blood Flow Metab. 2014; 34:380–388. [PubMed: 24326385]

16. Buckley EM, Parthasarathy AB, Grant PE, Yodh AG, Franceschini MA. Diffuse correlation spectroscopy for measurement of cerebral blood flow: future prospects. Neurophotonics. 2014; 1:011009. [PubMed: 25593978]
17. Carp SA, Dai GP, Boas DA, Franceschini MA, Kim YR. Validation of diffuse correlation spectroscopy measurements of rodent cerebral blood flow with simultaneous arterial spin labeling MRI; towards MRI-optical continuous cerebral metabolic monitoring. Biomed Opt Express. 2010; 1:553–565. [PubMed: 21258489]
18. Cheung C, Culver JP, Takahashi K, Greenberg JH, Yodh AG. In vivo cerebrovascular measurement combining diffuse near-infrared absorption and correlation spectroscopies. Phys Med Biol. 2001; 46:2053–2065. [PubMed: 11512610]
19. Culver JP, Durduran T, Furuya T, Cheung C, Greenberg JH, Yodh AG. Diffuse optical tomography of cerebral blood flow, oxygenation, and metabolism in rat during focal ischemia. J Cereb Blood Flow Metab. 2003; 23:911–924. [PubMed: 12902835]
20. Rice JE 3rd, Vannucci RC, Brierley JB. The influence of immaturity on hypoxic-ischemic brain damage in the rat. Ann Neurol. 1981; 9:131–141. [PubMed: 7235629]
21. Cuaycong M, Engel M, Weinstein SL, Salmon E, Perlman JM, Sunderam S, Vannucci SJ. A novel approach to the study of hypoxia-ischemia-induced clinical and subclinical seizures in the neonatal rat. Dev Neurosci. 2011; 33:241–250. [PubMed: 21952605]
22. Patel S, Pierce L, Ciardiello A, Hutton A, Paskewitz S, Aronowitz E, Voss H, Moore H, Vannucci S. Therapeutic hypothermia and hypoxia-ischemia in the term-equivalent neonatal rat: characterization of a translational pre-clinical model. Pediatr Res. 2014
23. Durduran T, Yodh AG. Diffuse correlation spectroscopy for non-invasive, micro-vascular cerebral blood flow measurement. Neuroimage. 2014; 85(pt 1):51–63. [PubMed: 23770408]
24. Roche-Labarbe N, Carp SA, Surova A, Patel M, Boas DA, Grant RE, Franceschini MA. Noninvasive optical measures of CBV, StO_2, CBF index, and $rCMRO_2$ in human premature neonates' brains in the first six weeks of life. Hum Brain Mapp. 2010; 31:341–352. [PubMed: 19650140]
25. Vannucci RC, Towfighi J, Heitjan DF, Brucklacher RM. Carbon-dioxide protects the perinatal brain from hypoxic-ischemic damage – an experimental study in the immature rat. Pediatrics. 1995; 95:868–874. [PubMed: 7761212]
26. De Ley G, Nshimyumuremyi JB, Leusen I. Hemispheric blood flow in the rat after unilateral common carotid occlusion: evolution with time. Stroke. 1985; 16:69–73. [PubMed: 3966269]
27. Ohshima M, Tsuji M, Taguchi A, Kasahara Y, Ikeda T. Cerebral blood flow during reperfusion predicts later brain damage in a mouse and a rat model of neonatal hypoxic-ischemic encephalopathy. Exp Neurol. 2012; 233:481–489. [PubMed: 22143064]
28. Qiao M, Latta P, Foniok T, Buist R, Meng S, Tomanek B, Tuor UI. Cerebral blood flow response to a hypoxic-ischemic insult differs in neonatal and juvenile rats. MAGMA. 2004; 17:117–124. [PubMed: 15538659]
29. Towfighi J, Mauger D, Vannucci RC, Vannucci SJ. Influence of age on the cerebral lesions in an immature rat model of cerebral hypoxia-ischemia: a light microscopic study. Brain Res Dev Brain Res. 1997; 100:149–160. [PubMed: 9205806]
30. Jensen EC, Bennet L, Hunter CJ, Power GC, Gunn AJ. Post-hypoxic hypoperfusion is associated with suppression of cerebral metabolism and increased tissue oxygenation in near-term fetal sheep. J Physiol. 2006; 572:131–139. [PubMed: 16484307]
31. McPhee AJ, Kotagal UR, Kleinman LI. Cerebrovascular hemodynamics during and after recovery from acute asphyxia in the newborn dog. Pediatr Res. 1985; 19:645–650. [PubMed: 3839577]
32. Rosenberg AA. Cerebral blood flow and O_2 metabolism after asphyxia in neonatal lambs. Pediatr Res. 1986; 20:778–782. [PubMed: 3737291]
33. Tichauer KM, Brown DW, Hadway J, Lee TY, St Lawrence K. Near-infrared spectroscopy measurements of cerebral blood flow and oxygen consumption following hypoxia-ischemia in newborn piglets. J Appl Physiol. 2006; 100:850–857. [PubMed: 16293704]
34. Charriaut-Marlangue C, Nguyen T, Bonnin P, Duy AP, Leger PL, Csaba Z, Pansiot J, Bourgeois T, Renolleau S, Baud O. Sildenafil mediates blood flow redistribution and neuroprotection after neonatal hypoxia-ischemia. Stroke. 2014; 45:850–856. [PubMed: 24473179]

35. Mujsce DJ, Christensen MA, Vannucci RC. Cerebral blood flow and edema in perinatal hypoxic-ischemic brain damage. Pediatr Res. 1990; 27:450–453. [PubMed: 2345670]

36. Dehaes M, Aggarwal A, Lin PY, Rosa Fortuno C, Fenoglio A, Roche-Labarbe N, Soul JS, Franceschini MA, Grant PE. Cerebral oxygen metabolism in neonatal hypoxic-ischemic encephalopathy during and after therapeutic hypothermia. J Cereb Blood Flow Metab. 2014; 34:87–94. [PubMed: 24064492]

37. Wintermark P, Hansen A, Warfield SK, Dukhovny D, Soul JS. Near-infrared spectroscopy versus magnetic resonance imaging to study brain perfusion in newborns with hypoxic-ischemic encephalopathy treated with hypothermia. Neuroimage. 2014; 85(pt 1):287–293. [PubMed: 23631990]

38. Gunn AJ, Gunn TR, de Haan HH, Williams CE, Gluckman PD. Dramatic neuronal rescue with prolonged selective head cooling after ischemia in fetal lambs. J Clin Invest. 1997; 99:248–256. [PubMed: 9005993]

39. Greisen G. Cerebral blood flow and oxygenation in infants after birth asphyxia. Clinically useful information? Early Hum Dev. 2014; 90:703–705. [PubMed: 25028135]

40. Tichauer KM, Wong DYL, Hadway JA, Rylett RJ, Lee T-Y, St Lawrence K. Assessing the severity of perinatal hypoxia-ischemia in piglets using near-infrared spectroscopy to measure the cerebral metabolic rate of oxygen. Pediatr Res. 2009; 65:301–306. [PubMed: 19033882]

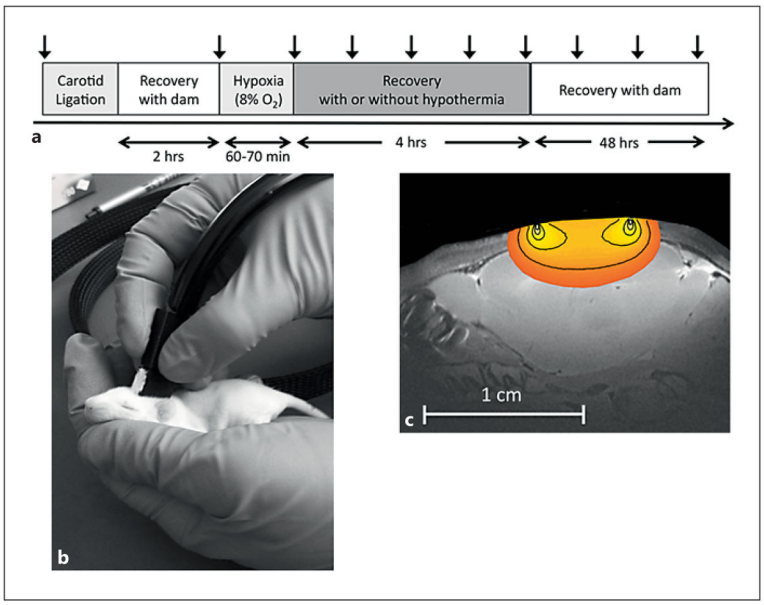

Fig. 1.

a Vertical arrows denote time points of DCS measurements. **b** DCS measurement on a rat pup. The pups were gently restrained and the optical sensor was held over the right and left hemispheres. DCS measurements of CBF_i were made over each hemisphere, lasting approximately 30 s. **c** Depth sensitivity of the DCS measurements to the neonatal rat brain.

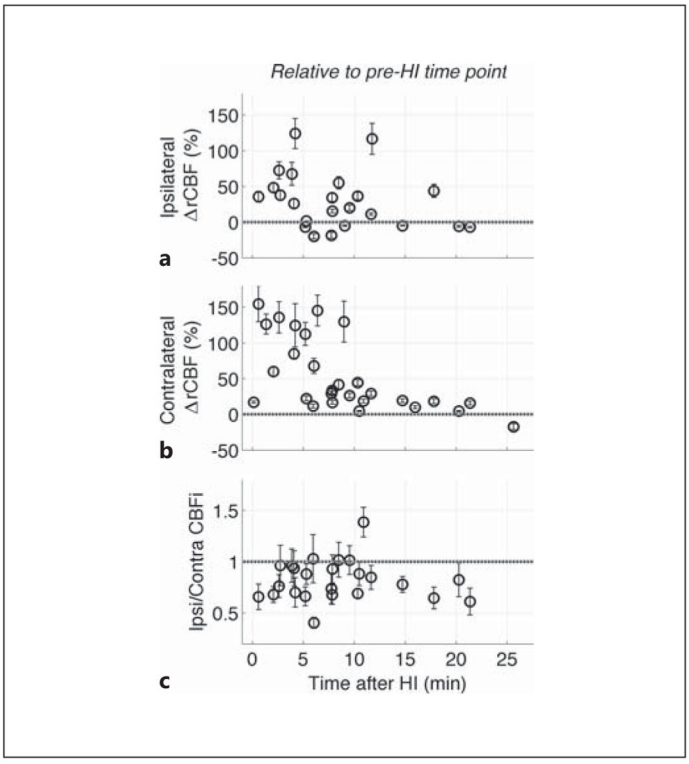

Fig. 2.

Immediate relative changes in CBF (ΔrCBF) after HI from postligation levels in the ipsilateral (**a)** and contralateral (**b)** hemispheres. **c** Ratio of ipsilateral-to-contralateral CBF_i immediately after HI. Data includes all pups from the HI-N group, as well as a subset of pups in the HI-TH groups that were measured before the initiation of cooling. The grey dotted horizontal line indicates no change from postligation, pre-HI levels (**a, b)** or no difference between ipsilateral and contralateral CBF_i (**c)**. CBF_i data was obtained sequentially, i.e. each rat was measured at a slightly different time point.

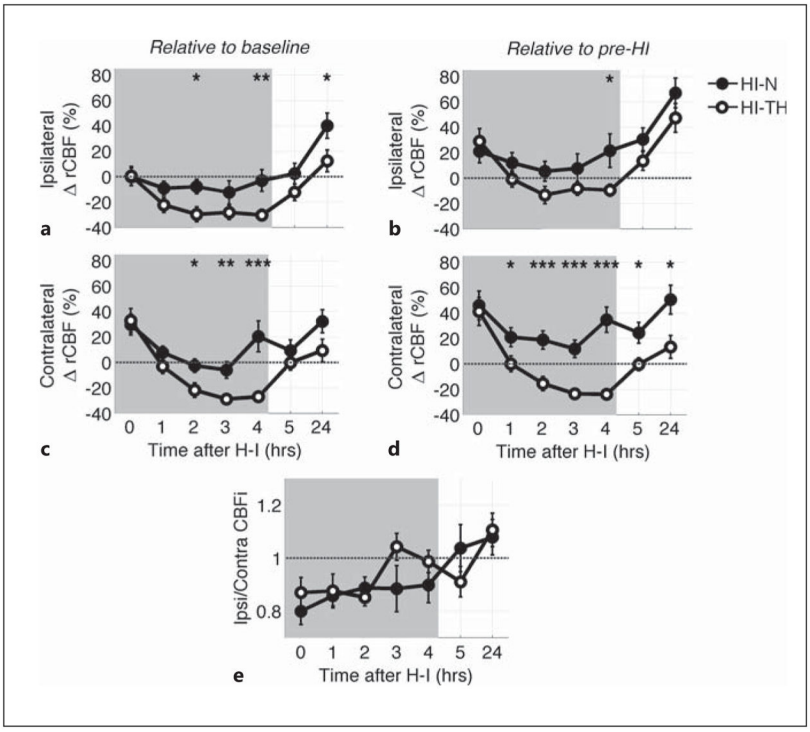

Fig. 3.

Mean (SEM) relative change in CBF (ΔrCBF) from preligation levels (**a, c)** and from postligation levels (**b, d)** within the first 24 h after HI for HI-N and HI-TH animals in ipsilateral (**a, b)** and contralateral (**c, d)** hemispheres. **e** Ratio of ipsilateral-to-contralateral CBF_i during this recovery time period. HI-TH animals were actively cooled in a hypothermic chamber during the time period shaded in gray, whereas HI-N animals were in a normothermic chamber during this time period. After the 4-hour time point, the animals were returned to the dam. The grey dotted horizontal line indicates no change in CBF_i (**a–d)** or no difference between hemispheres (**e)**. Significant differences between the HI-N and HI-TH groups were determined by an unpaired t-test. * $p < 0.05$; ** $p < 0.01$; *** $p < 0.001$.

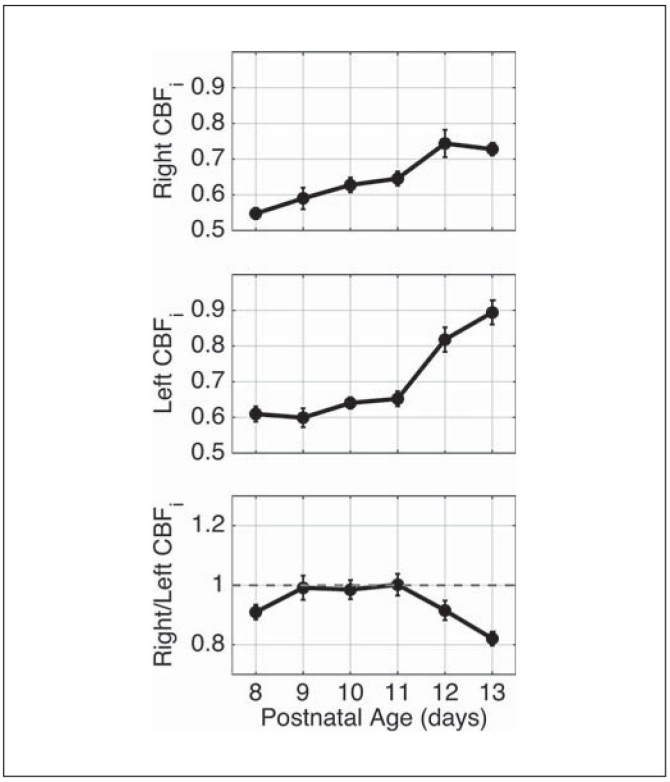

Fig. 4.

Mean (SEM) CBF_i (in units of 10^{-5} mm^2/s) as a function of age in 24 healthy control rat pups measured daily from P8 to P13. The animals were measured at approximately the same time every day.

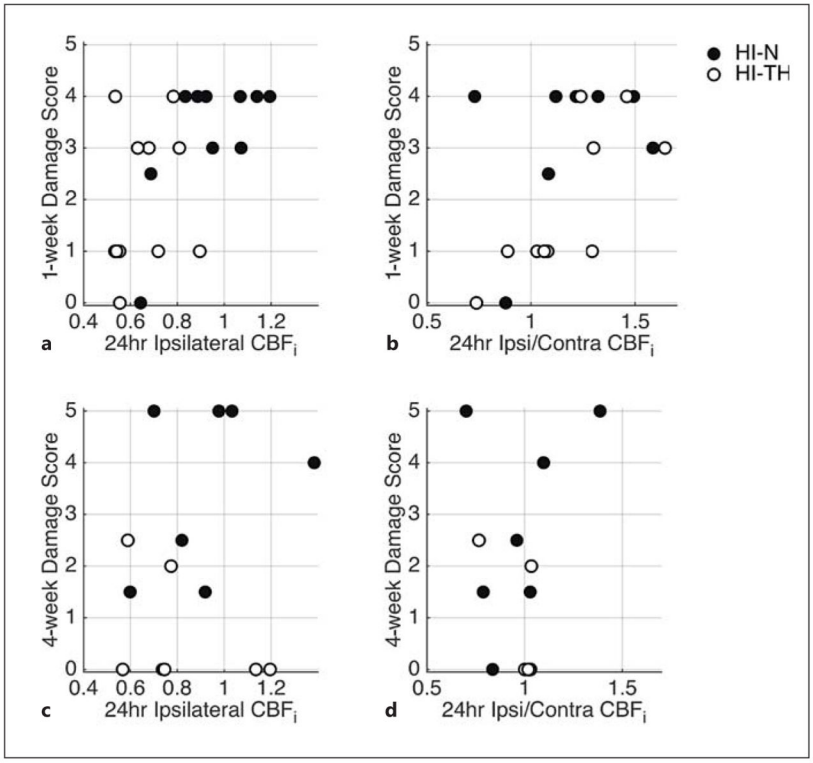

Fig. 5.

Relationship between ipsilateral CBF_i as well as ipsilateral-to-contralateral CBF_i ratio measured 24 h after HI with 1-week (**a, b)** and 4-week (**c, d)** injury scores for HI-N and HI-TH animals. The 1-week injury scores were significantly positively correlated with ipsilateral CBF_i ($R = 0.55$, $p = 0.009$) and ipsilateral-to-contralateral CBF_i ratio ($R = 0.51$, $p = 0.030$).

Table 1

Relative changes in CBF after HI

	Ipsilateral ΔrCBF (%)		Contralateral ΔrCBF (%)		Ipsilateral-to-contralateral CBF_i ratio	
	HI-N	HI-TH	HI-N	HI-TH	H I-N	HI-TH
After HI, h						
0	−0.1 (7.0)	−0.6 (−7.4)	29.7 (8.3)[b]	32.9 (9.4)[b]	0.80 (0.05)[c]	0.87 (0.06)[a]
1	−9.1 (5.5)	−22.3 (5.9)[c]	7.8 (5.0)	−3.1 (5.6)	0.86 (0.04)[c]	0.88 (0.06)[a]
2	−7.9 (5.7)[d]	−29.7 (5.7)[c]	−2.6 (5.3)[d]	−21.7 (5.7)[c]	0.89 (0.04)[a]	0.85 (0.03)[c]
3	−12.4 (9.3)	−28.2 (5.6)[c]	−5.9 (6.5)[e]	−28.8 (2.9)[c]	0.88 (0.09)	1.04 (0.05)
4	−3.1 (8.5)[e]	−30.3 (4.5)[c]	20.4 (12.1)[f]	−27 (3.6)[c]	0.90 (0.07)	0.99 (0.04)
5	2.4 (8.1)	−12.3 (6.5)[a]	9.3 (8.4)	−0.1 (6)	1.04 (0.09)	0.91 (0.06)[a]
24	40.1 (10.0)[c,d]	12.4 (8.5)	32.3 (9.1)[b]	9.3 (8.9)	1.08 (0.07)	1.11 (0.06)
48	−8.0 (11.7)	−8.7 (6.9)	8.1 (9.9)[d]	46.7 (21.3)	0.85 (0.09)	0.72 (0.03)[b]

Data are reported as means (SEM). Relative change in CBF (ΔrCBF) from baseline levels and ipsilateral-to-contralateral CBF_i ratios for each time point after HI. Data are reported for the HI-N and HI-TH groups separately.

[a] $p < 0.05$,

[b] $p < 0.01$,

[c] $p < 0.001$ compared to baseline, before ligation;

[d] $p < 0.05$,

[e] $p < 0.01$,

[f] $p < 0.001$ compared to the HI-TH group at the same time point.